SVU-International Journal of Engineering Sciences and Applications (2024) 5(2): 1-6
Print ISSN 2785-9967 | Online ISSN 2735-4571
DOI 10.21608/svusrc.2023.194531.1100

Investigation of Xiaomi 11T Single-Frequency GPS Positioning for Static Applications

Mohamed Abdelazeem[1, 2], Hussain A. Kamal[2,], and Amr M. Wahaballa[2]

Abstract Currently, the raw Global Navigation Satellites Systems (GNSS) measurements from android smartphone are widely used in precise positioning and mapping applications. The objective of our paper is to investigate the accuracy of low-cost single-frequency GPS Precise Point Positioning (PPP) using Xiaomi 11T smartphone. The single-frequency GPS PPP accuracy is evaluated for static applications in post processing mode. Two-hour static GPS measurements are acquired from both Xiaomi 11T smartphone and Leica GS15 geodetic receiver over Faculty of Engineering, Aswan, Egypt, reference station, spanning two different days. Then, the observations are processed using two different PPP solutions, namely code-only and code and carrier phase PPP solutions. All data are processed using the Net-Diff GNSS software. To account for satellite orbits, clock and ionospheric errors, the International GNSS Service (IGS) final products are used. The PPP positioning accuracy and convergence time obtained through the Xiaomi 11T smartphone are compared with those obtained through the Leica GS15 geodetic receiver. It is shown that the single-frequency GPS PPP solution has decimeter-level positioning accuracy in easting and northing components for 30-min, 1-hour, 1.5-hour and 2-hour time windows. For the height component, meter-level positioning accuracy is obtained for 30-min, 1-hour time windows and centimeter-level for 1.5-hour and 2-hour time windows.

Keywords: GNSS, Xiaomi 11T smartphone, Precise Point Positioning (PPP).

1 Introduction

Recently, there is a growing interest in using low-cost technologies such as smartphones and tablets for positioning and mapping applications. The Android 7 (Nougat) operating system allows users to obtain GNSS raw observations (e.g., pseudo-range and carrier-phase measurements) through mobile applications [1]. In 2017, Geo++ released an application called Geo++ RINEX Logger, providing raw GNSS observations directly in RINEX format [2]. Xiaomi released the first dual-frequency GNSS smartphone in 2018, which is Mi 8 smart phone. Mi 8 smartphone has a Broadcom BCM47755 chip installed, which enables several GNSS features [3]. The availability of multi GNSS features smartphones and accessibility of GNSS raw data was a breakthrough for GNSS smartphones precise positioning applications. Smartphones are similar to geodetic receiver in tracking multi-frequency multi-constellation GNSS satellites, but their carrier-to-noise ratio are worse [4]. The carrier-to-noise ratio refers to the ratio of the average power of the carrier signal received at the receiver end to the average power of the noise when the signal is interfered in the process of propagation. The measurement's noise level is reflected in the carrier-to-noise ratio value [5], [6]. Therefore, GNSS data quality is a crucial issue for smartphones observations.

The performance of smartphone positioning has been studied by a number of researchers. The accuracy of Single Point Positioning (SPP) using the Nexus 9 tablet code measurements has been found in meter-level accuracy [7]. [8] investigated the accuracy of Xiaomi Mi 8 using dual-frequency GPS/Galileo observations in both post processing and real-time PPP modes. It has been found that the positioning accuracy was in centimeter-level. Also, decimeter-level positioning accuracy for static applications and meter-level accuracy for kinematic applications has been obtained using single-frequency GPS/GLONASS Xiaomi Mi 8 observations [9]. In addition, decimeter-level accuracy for horizontal positioning has been achieved using an improved PPP model [6].

Received: 17 February 2023 / Accepted: 28 December 2023

 Corresponding Author: Hussain A. Kamal HussainAhmed@eng.aswu.edu.eg
1.Civil Engineering Department, College of Engineering, Prince Sattam bin Abdulaziz University, Al-Kharj 16273, Saudi Arabia
2.Civil Engineering Department, Faculty of Engineering, Aswan University, Aswan 81542, Egypt

The objective of our research is to investigate the positioning accuracy of single-frequency GPS PPP solution using Xiaomi 11T in static mode. Xiaomi 11T is a multi-frequency multi-constellation smartphone (i.e., L1/L5 GPS, E1/E5a Galileo, L1 GLONASS, L1 Bei Dou). Xiaomi 11T GNSS features tested by GPSTEST mobile application [10]. Our choosing criteria for Xiaomi 11T are availability, reasonable price compare with other smartphones have same GNSS features, battery capacity (5000mAh) and finally great storage capacity (256 GB) [11]. The observations are processed using two different PPP solutions, namely code-only and code and carrier phase PPP solutions. The PPP positioning accuracy is evaluated for static applications in post processing mode. The single-frequency GPS PPP positioning accuracies are validated with this obtained from Leica GS15 geodetic receiver.

2 Single-Frequency PPP Mathematical Model

The GPS only observation equations are represented as follows [12]:

$$\boldsymbol{p_1(t) = \rho(t, t-\tau) + c.[dt_r(t) - dt^s(t-\tau)] + c.[d_r(t) + d^s(t-\tau)]_1 + T + I_1 + \varepsilon_{p1}} \quad (1)$$

$$\boldsymbol{\Phi_1(t) = \rho(t, t-\tau) + c.[dt_r(t) - dt^s(t-\tau)] + c.[\delta_r(t) + \delta^s(t-\tau)]_1 + \lambda_1.[\phi_r(t_0) - \phi^s(t_0)]_1 + \lambda_1 N_1 + T - I_1 + \varepsilon_{\Phi 1}} \quad (2)$$

where p_1 and Φ_1 are pseudo-range and carrier measurement on L_1 frequency respectively; $\rho(t, t-\tau)$ is the true geometric range from the antenna phase center of the receiver at reception time t to the antenna phase center of the satellites at transmission time $(t-\tau)$; C is speed of light in vacuum; $dt_r(t)$ and $dt^s(t-\tau)$ are receiver clock errors at reception time and satellite clock error at transmitting time respectively; $d_r(t)$ and $d^s(t-\tau)$ are frequency-dependent code hardware delays for the receiver at reception time and the satellite at transmitting time, respectively; $\delta_r(t)$ and $\delta^s(t-\tau)$ are frequency dependent carrier phase hardware delays for the receiver at reception time and the satellite at transmitting time, respectively; T is tropospheric delay; I_1 is ionospheric delay on L_1 frequency; λ_1 is wavelength on L_1 frequency; $\phi_{r1}(t_0)$ and $\phi^s{}_1(t_0)$ are frequency dependent initial fractional phase biases in the receiver and satellite channels at initial time t_0; N_1 is carrier-phase ambiguity parameter on L_1 frequency and finally $\varepsilon_{(p_1,\Phi_1)}$ are multipath and measurement noise for pseudo-range and carrier phase measurements in meter.

For satellites orbit and clock errors can be accounted using final IGS products. The IGS satellites clock correction works as following [13]:

$$\boldsymbol{dt^s{}_{IGS} = dt^s - (2.546\, d^s_{p1} - 1.546\, d^s_{p2})} \quad (3)$$

where d^s_{p1} and d^s_{p2} are the satellite hardware delays for p_1 and p_2. By substituting equation (3) into equation (1), the code observation equation can be written as follows:

$$\boldsymbol{p_1(t) = \rho + c.dt'_r - c.[dt^s{}_{IGS} + 1.546\, DCB^s_{p_1p_2}] + T + I_1 + \varepsilon_{p1}} \quad (4)$$

where, $(DCB^s_{p_1p_2} = d^s_{p1} - d^s_{p2})$ is differential code bias; $(dt'_r = [dt + d_{p1}]_r)$ is the sum of the receiver clock error and the code hardware delay for the receiver. For carrier phase observation equation, it takes the following form:

$$\boldsymbol{\Phi_1(t) = \rho + c.dt'_r - c.\left[dt^s{}_{IGS} + 1.546\, DCB^s_{p_1p_2}\right] + T + A - I_1 + \varepsilon_{\Phi 1}} \quad (5)$$

where A is ambiguity parameter which is the sum of the integer ambiguity, phase hardware delay for both satellite and receiver, and initial fractional phase bias for both satellite and receiver. Tropospheric delay is divided into dry tropospheric delay and wet tropospheric delay. The dry tropospheric delay can be accounted for using empirical model, while the wet delay is estimated as unknown parameter. For the ionospheric delay, it can be accounted for using the IGS global ionospheric map (GIM). For parameter estimation, the unknown parameters for single-frequency PPP model are receiver coordinates, receiver clock, wet tropospheric component and ambiguity parameter.

3 GPS Data Processing

Static GPS data sets have been collected on Day of Year (DOY) 151 and 153 over Aswan Control Point (Aswan CP) in Aswan faculty of engineering using both Xiaomi 11T smartphone and Leica GS 15 geodetic receiver as it shown in Figure 1. It should be mentioned that the 2-hour dataset of the smartphone is collected first and then the 2-hour dataset of the geodetic receiver is collected. The smartphone's time window is from 04:30AM to 6:30AM local time, while the geodetic receiver's time window is from 7:00 AM to 9:00 AM local time. The Geo++RINEX android application has been used in order to collect GNSS data with smartphone.

(a)

(b)

Fig.1 Xiaomi 11T (a) and Leica GS15 (b) centring over Point.

To investigate the quality of the collected observations, the carrier-to-noise ratio has been evaluated for both smartphone and geodetic receiver. Figure 2 illustrates the mean values of carrier-to-noise ratio for GPS signals. Similar results have been obtained for both examined days. Therefore, only results on DOY 151 is given as examples. It can be seen that the number of the tracked satellites by both smartphone and geodetic receiver is different. This is due to the difference in time window. In addition, the mean carrier-to-noise ratio for GPS L1 signal with the geodetic receiver is greater than 40 dBHz for all satellites. On the other hand, the mean value for Xiaomi 11T is less than 30 dBHz. An except is for satellites G24, G15, G13, G12, G11, G06 and G02. The minimum value of carrier-to-noise ratio is for satellites G32 and G05, which is less than 20 dBHz. Thus, it is expected poor quality of carrier measurements data from these two satellites.

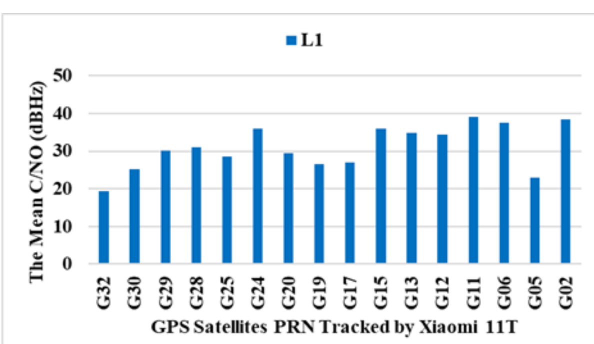

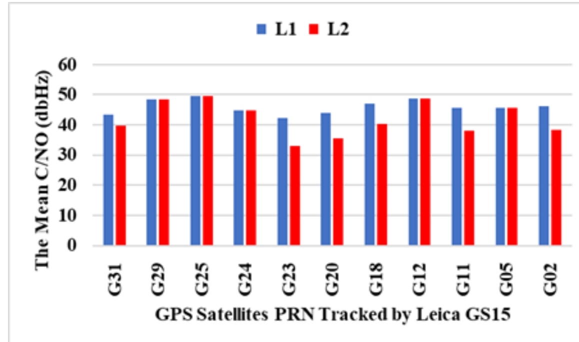

Fig.2 The mean carrier-to-noise ratio of L1 and L2 GPS satellites for Xiaomi 11T and Leica GS15, respectively.

The observation files from both smartphone and geodetic receiver have been processed using the Net-Diff GNSS software [14] using single-frequency PPP solution in post processing mode. Two single-frequency PPP solutions has been used, namely code-only and code and carrier phase PPP solutions. To account for satellite orbit, clock and ionospheric errors, the final IGS products have been used [15]. Table 1 summarizes the PPP processing parameters.

Table 1 Net-Diff software GNSS PPP processing parameters

Parameter	**Solution**
Satellite orbit , Satellite clock , GNSS BSX and Ionospheric Model	[Final] IGS
Tropospheric model Meteorological Model Mapping Function	Saastamoinen GPT VMF1
Cut of angel	10 degrees
Satellite & Receiver Antenna Phase Center Offset	ANTEX files
Observation Type	Code + Carrier/ Code
Frequency	L1
Processing Mode	Static
Stochastic Model	Elevation Dependent
Cycleslip detection	Yes
Smooth	No
Parameter estimation method	Kalman Filter

4 Result and Analysis

In our paper, single–frequency GPS observations from both devices smartphone and geodetic receiver are processed in post processed mode using single-frequency PPP solution. Two different single-frequency PPP solutions are used, including code-only (i.e., S(P) and G(P) for smartphone and geodetic receiver, respectively) and code and carrier phase (i.e., S(P+C) and G(P+C) smartphone and geodetic receiver, respectively).

The known coordinates of our selected control point are used as references. The convergence time and positioning accuracy are investigated. Figure 3 and 4 shows the positioning errors in easting, northing and height components for both smartphone and geodetic receiver on both examined days. It Is shown that the positioning solution obtained from the smartphone is converged in easting direction faster than the northing direction. In addition, smartphone code-only solution is better than the code and carrier solution. This is due to that the quality of carrier measurements collected by the smartphone.

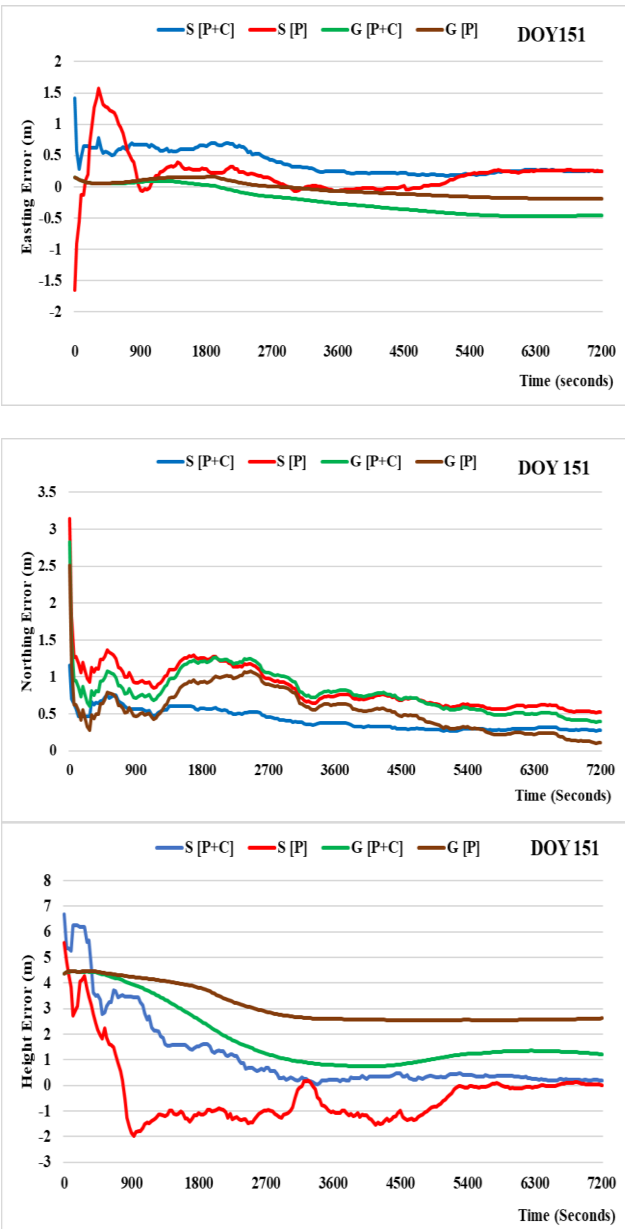

Fig.3 Positioning errors for Xiaomi 11T and Leica GS15 using the two PPP solutions on DOY 151.

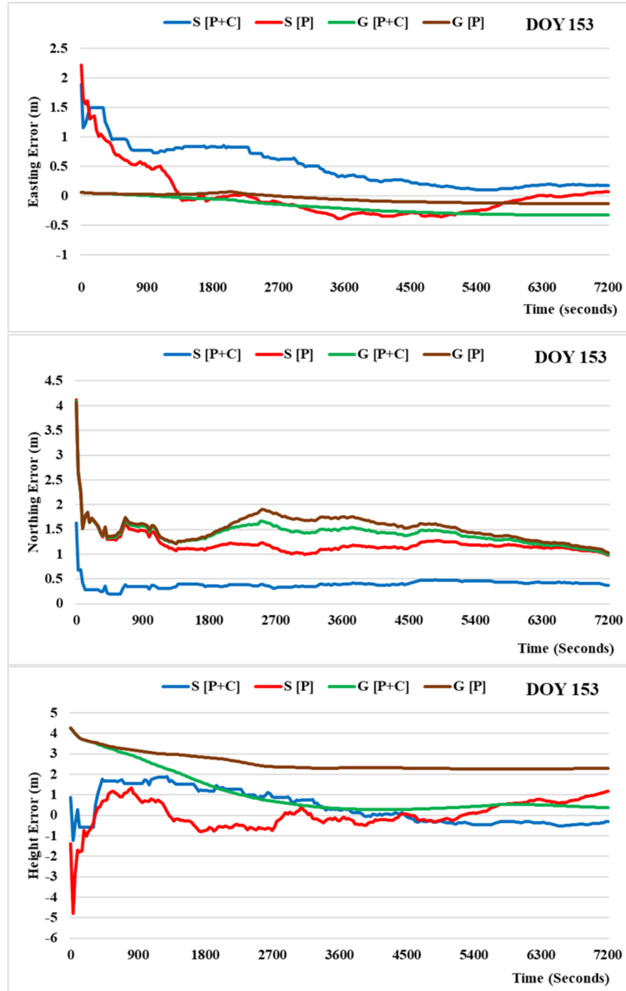

Fig.4 Positioning errors for Xiaomi 11T and Leica GS15 using the two PPP solutions on DOY 153.

To further evaluate the Xiaomi 11T positioning accuracy, the Root Mean square Error (RMSE) is determined as it shown in figures 5. It can be seen that RMSE values for the smartphone is about 0.39, 0.47 and 1.35 meter in easting, northing and height components, respectively, for code-only solution. For the code and carrier solution, it is about 0.43, 0.44 and 1.88 meter in easting, northing and height components, respectively. Additionally, for the geodetic receiver, the RMSE values are about 0.13, 0.24 and 3.17 meter in easting, northing and height component, respectively, for code-only solution. For code and carrier solution, the RMSE values are 0.31, 0.13 and 2.22 meter in easting, northing and height, respectively. It is also shown that, for the height component, the RMSE of Xiaomi 11T is superior to that of the Leica GS15. This might be attributed to the ionosphere effect as the observation time for the smartphone and the geodetic receiver is different.

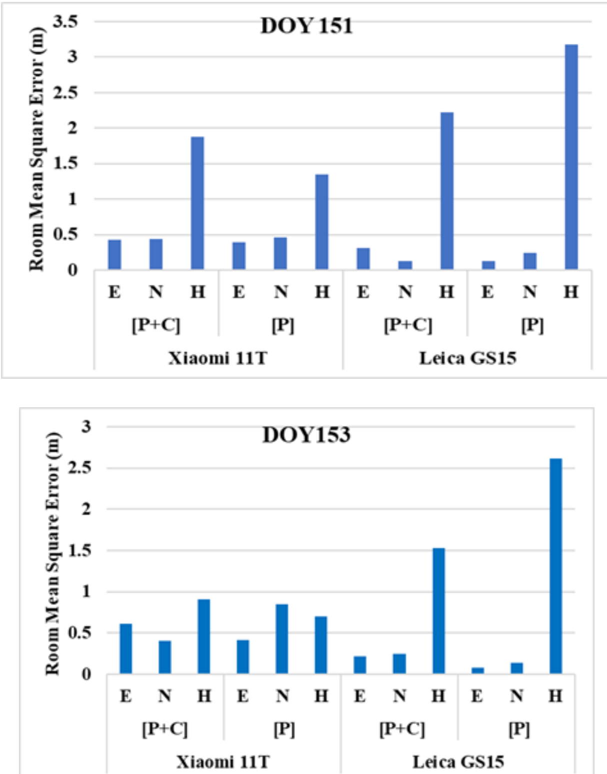

Fig.5 Root Mean Square Error for PPP Positioning.

The positioning accuracy for single-frequency PPP solutions obtained from both Xiaomi 11T and Leica GS15 is given in Table 2 and Table 3. It is shown that the positioning accuracy of the two PPP solutions is in decimeter-level in easting and northing components for 30-min, 1-hour, 1.5-hour and 2-hour time windows for both smartphone and geodetic receiver. For the height component, meter-level positioning accuracy is obtained from the two solutions for both smartphone and geodetic receiver in different time windows. From the obtained results, it can be said that Xiaomi 11T smartphone's single-frequency GPS PPP positioning accuracy is suitable for some static applications that require centimeter-level horizontal position accuracy.

Table 2 Xiamoi 11T position accuracies for 30-minute, 1-hour, 1.5-hour and 2-hour time windows.

Time (Minutes)	Xiaomi 11T					
	[P+C]			[P]		
	E	N	H	E	N	H
DOY 151						
30	0.67	0.58	1.51	0.30	0.68	1.18
60	0.25	0.38	0.22	0.06	0.37	1.02
90	0.20	0.30	0.42	0.20	0.34	0.10
120	0.25	0.28	0.18	0.25	0.24	0.02
DOY 153						
30	0.83	0.36	1.20	0.04	0.76	0.73
60	0.33	0.40	0.25	0.36	0.76	0.26
90	0.11	0.46	0.46	0.25	0.73	0.12
120	0.18	0.37	0.29	0.07	0.61	1.18

Table.3 Leica GS15 position accuracies for 30-minute, 1-hour, 1.5-hour and 2-hour time windows.

Time (Minutes)	Leica GS15					
	[P+C]			[P]		
	E	N	H	E	N	H
DOY 151						
30	0.03	0.05	2.57	0.16	0.28	3.83
60	0.27	0.06	0.80	0.07	0.18	2.59
90	0.44	0.05	1.24	0.16	0.26	2.56
120	0.45	0.13	1.22	0.19	0.29	2.62
DOY 153						
30	0.05	0.24	1.51	0.05	0.03	2.82
60	0.21	0.38	0.34	0.06	0.23	2.31
90	0.30	0.15	0.44	0.12	0.09	2.26
120	0.32	0.01	0.38	0.13	0.04	2.31

5 Conclusion

In this research, the positioning accuracy of single-frequency GPS PPP solution using Xiaomi 11T smartphone has been investigated. Static GPS observations have been collected using both Xiaomi 11T and Leica GS15 geodetic receiver. Two different single-frequency PPP solutions have been used in order to process the observations in post processed mode namely code-only and code and carrier phase PPP solutions. It has been found that the smartphone's single-frequency GPS PPP solution has decimeter-level positioning accuracy in easting and northing components for 30-min, 1-hour, 1.5-hour and 2-hour time windows. For the height component, meter-level positioning accuracy is obtained for 30-min, 1-hour time windows and centimeter-level for 1.5-hour and 2-hour time windows.

Acknowledgment

Great thanks for Mr. Yize Zhang for providing Net-Diff software and for helpful advice and employees of surveying laboratory in Aswan Faculty of Engineering, Aswan , Egypt.

References

[1] Steve Malkos, "Google to provide raw GNSS measurements," Jul. 10, 2016. https://www.gpsworld.com/google-to-provide-raw-gnss-measurements/ (accessed Apr. 20, 2022).

[2] Geo++ GmbH, "Geo++ RINEX Logger." 2017. Accessed: May 1st, 2023. [Online]. Available: https://play.google.com/store/apps/details?id=de.geopp.rinexlogger

[3] GPS World Staff, "Dual-frequency GNSS smartphone hits the market," Jun. 11, 2018. https://www.gpsworld.com/dual-frequency-gnss-smartphone-hits-the-market/ (accessed May 1st, 2023).

[4] J. Bruno, F. Darugna, K. Bolmgren, J. B. Wübbena, C. Mitchell, and M. Schmitz, "Quality analysis of dual-frequency smartphone-based ionospheric tec

measurements: What can be achieved?," *Annals of Geophysics*, vol. 63, pp. 1–14, 2020, https://doi.org/10.4401/ag-8517 .

[5] R. W. G. and R. T. C. for M. S. S. C. 104 (RTCM-S. International GNSS Service (IGS), *RINEX The Receiver Independent Exchange Format Version 3.03*. 2015. Accessed: May 1st, 2023. [Online]. Available: https://igs.org/pub/data/format/rinex303.pdf

[6] G. Wang, Y. Bo, Q. Yu, M. Li, Z. Yin, and Y. Chen, "Ionosphere-constrained single-frequency ppp with an android smartphone and assessment of gnss observations," *Sensors (Switzerland)*, vol. 20, no. 20, pp. 1–15, Oct. 2020, https://doi.org/10.3390/s20205917 .

[7] J. Gim and K. Park, "Comparison of Positioning Accuracy Using the Pseudorange from Android GPS Raw Measurements," *J. Adv. Navig. Technol*, vol. 21, no. 5, pp. 514–519, 2017, https://doi.org/10.12673/jant.2017.21.5.514 .

[8] A. Elmezayen and A. El-Rabbany, "Precise point positioning using world's first dual-frequency GPS/galileo smartphone," *Sensors (Switzerland)*, vol. 19, no. 11, Jun. 2019, https://doi.org/10.3390/s19112593 .

[9] M. A. Rabbou, M. Mahmoud, and A. El Shazly, "Performance Evaluation of Single Frequency PPP using Smartphone's Raw GNSS Observations," *Al-Azhar University Civil Engineering Research Magazine (CERM)*, vol. 43, no. 2, Apr. 2021.

[10] BarbeauDev, "GPSTest." 2022. Accessed: May 1st, 2023. [Online]. Available: https://play.google.com/store/apps/details?id=com.android.gpstest&hl=en_US&gl=US

[11] Hannah Cowton, "Xiaomi 11T review," Nov. 01, 2021. https://www.techadvisor.com/article/722760/xiaomi-11t-review.html (accessed May 1st, 2023).

[12] Peter J. G. Teunissen and Alfred Kleusberg, *GPS for Geodesy*, 2nd ed. Berlin, Heidelberg: Springer Berlin Heidelberg, 1998. https://doi.org/10.1007/978-3-642-72011-6 .

[13] M. A. El-Rahman and A. El-Rabbany, "Performance Evaluation of USTEC Product for Single-Frequency Precise Point Positioning," *GEOMATICA*, vol. 67, no. 4, pp. 253–257, 2013, https://doi.org/10.5623/cig2013-051 .

[14] YizeZhang, " Net_Diff ." 2022. Accessed: May 30, 2022. [Online]. Available: https://github.com/YizeZhang/Net_Diff

[15] IGS, "International GNSS Service (IGS)," 2022. https://igs.org/ (accessed May 1st, 2023).